

Disorder-Induced Topological Defects in a $d = 2$ Elastic Medium at Zero Temperature

A. Alan Middleton

Department of Physics, Syracuse University, Syracuse, New York 13244

(March 13, 1998)

The density and correlations of topological defects are investigated numerically in a model of a $d = 2$ elastic medium subject to a periodic quenched random potential. The computed density of defects decreases approximately exponentially with the defect core energy. Comparing the defect-free ground state with the ground state with defects, it is found that the difference is described by string-like excitations, bounded by defect pairs, which have a fractal dimension of 1.250 ± 0.003 . At zero temperature, the disorder-induced defects screen the interaction of introduced vortex pairs.

74.60.Ge, 75.10.Nr, 02.70.Lq, 02.60.Pn

A diverse set of physical phenomena, including vortex lattices in superconductors, incommensurate charge density waves, and crystal growth on a disordered substrate, have been modeled as elastic media subject to a pinning potential due to quenched disorder [1–3]. A possible difficulty in applying these purely elastic models is their failure to take into account the possible effect of defects in the elastic medium [1,4,5]. In general, the importance of defects have been difficult to analyze analytically, though recent numerical simulations and analytical arguments have indicated that defects significantly change the $d = 2$ system, but have less effect in $d = 3$ [4,5].

In this paper, I present results on the effects of scalar defects on the ground state of a model of a $d = 2$ elastic medium subject to a disordered pinning potential. Using variants of combinatorial techniques that have been applied [6–8] to the study of the elastic model without defects, it is possible to exactly calculate the finite-size ground states of models that allow for defects in the scalar displacement variable. By comparing configurations with and without defects, the change in ground state due to the introduction of defects is found to be confined to “strings” that connect defects. The fractal dimension of these strings is computed to be $1.250(3)$. The effects of the defects on the long-range response are calculated by the introduction of a *fixed* pair of defects into the elastic medium with defects. As the system size increases, the cost of introducing the fixed pair goes to a constant (rather than growing logarithmically), indicating that the defects screen the long-range interaction at long scales.

In models of d -dimensional elastic media with scalar displacement subject to a pinning potential periodic in the direction of displacement, there are two length scales that separate distinct behaviors [1,4]. For lengths less than the pinning length ξ_P , the elastic energies for deformation are typically larger than the pinning energies, so that the displacement in a region of volume ξ_P^d can be represented as a single scalar variable h , with the pinning energy periodic in h . For length scales greater than ξ_P , the

pinning energy dominates and there are many metastable states. In a medium that allows for the creation of defects (in the $d = 2$ case considered in this paper, these defects are point vortices), there is a length scale ξ_V describing the typical separation of vortices. The vortices themselves are described by their location to within ξ_P [1,4]. In this work, the lattice constant corresponds to the length scale ξ_P and the distance ξ_V is controlled by a vortex core energy E_c .

A model for interfaces and defects in $d = 2$ can be based upon the properties of matchings and their height representations. Given an undirected graph $G = (V, D)$, with vertices V and edges D , a matching $M \subseteq D$ is a set of edges such that each vertex belongs to at most one edge in M . The graphs of interest here will be bipartite (with subsets of vertices A and B and all edges connecting A - and B -vertices), with equal numbers of vertices in each sublattice, and allow for complete matchings, where each vertex is a member of exactly one edge. In particular, consider a hexagonal lattice with $L \times L$ two-vertex unit cells. There exists a one-to-one mapping between complete matchings on this lattice, minimally frustrated states of an antiferromagnetic Ising model on a triangular lattice, and a solid-on-solid height representation [9]. Fig. 1 indicates the mapping between matchings and a height representation. In the case of a partial matching, an equal number of A - and B -vertices are unmatched. The uncovered vertices correspond to defects (vortices or screw dislocations) in the height representation. The rules for calculating the height can still be applied locally, but are inconsistent on any loop containing an unequal number of A and B defects. Unmatched vertices have a positive (negative) sign, if the vertex is a member of the B (A) sublattice, respectively, as indicated in Fig. 1.

Consider the case of a complete matching M , where there is a well-defined interface corresponding to M . In the absence of quenched disorder, the energy of the interface is independent of the height configuration, so all matchings appear with equal weight, and the thermally-averaged height-height correlations $\langle [h(\vec{r}) - h(\vec{0})]^2 \rangle$ grows as $\sim \ln(r)$ at all temperatures T [9]. In the

presence of quenched disorder, this is no longer true at low temperatures. Theoretical calculations [1,10] predict that the 2+1-dimensional model at low temperature T has a correlation function that grows as $\sim \ln^2(r)$. This has been confirmed in the $T \rightarrow 0$ limit by numerical calculations using the complete matching representation and other methods [6,8]. The energy can be calculated in the matching representation as $E = -\sum_{e \in M} w_e$, where w_e are randomly chosen weights associated with each edge (dimer.) Maximizing the total weight minimizes the energy. When the corresponding interface in the height representation is translated by 3 units in the height direction, the dimer configuration is unchanged, so that the energy is periodic in global height shifts.

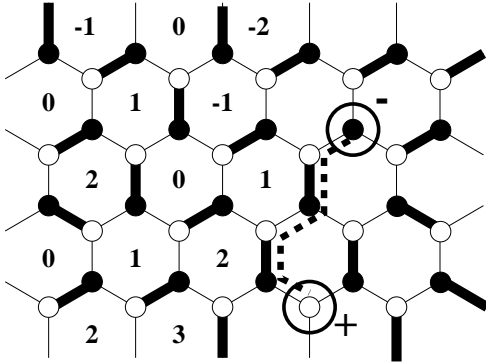


FIG. 1. Rules for assigning heights to matchings on a hexagonal lattice. A- (B-) vertices are shown as filled (unfilled) circles and matched edges are heavy line segments. All but the two circled vertices are matched. Heights h are defined at the centers of the hexagons. When crossing a matched edge from an A to a B vertex in the ccw direction about the A vertex, h increases by 2; if the edge is unmatched, h decreases by 1. A locally consistent definition of h is shown on the left side of the figure. The right side of the figure exhibits defects. The unmatched vertex on the A (B) sublattice correspond to a negative (positive) vortex. The dashed line indicates a possible path for a defect string that connects two defects; if this were the defect string, then in the ground state with no defects, the unmatched edges along this path would become matched and the matched edges would be removed.

In the case of an incomplete matching, there is no longer a uniquely defined height variable corresponding to displacements of the $d = 2$ elastic medium. An energy for the dimer configuration can then be assigned which is consistent with (1) a local pinning energy where vertices are covered by dimers in M and (2) a defect energy for vertices that are not the endpoints of dimers in M :

$$E = N_c E_c - \sum_{e \in M} w_e, \quad (1)$$

where N_c is the number of non-covered vertices and E_c is the core cost of a defect. Minimizing E in Eqn. (1) gives the $T = 0$ configuration for the elastic medium

with defects that have an associated core energy. Over local regions where the height is well defined, the energy is still periodic in the height (displacement) variable.

Ground-state configurations were found using two algorithms that solve maximum-weight bipartite matching (MWBM.) The first algorithm uses a heuristic developed by C. Zeng [11], implemented in the LEDA library of algorithms [12], to directly determine the (partial) matching that maximizes the sum in Eqn. (1). The second algorithm, using almost identical processor time and less memory, is based upon finding a maximum-weight *complete* matching in a modified graph, where vertices are duplicated and extra edges of weight $2E_c$ and of weight zero are added to the original edge set. A complete matching algorithm such as the cost-scaling assignment (CSA) algorithm by Kennedy and Goldberg [13] can then be used to find a complete matching on this augmented graph. Matched vertices in the augmented graph which correspond to edges in the original graph give the partial matching in the original graph that minimizes E . These algorithms take 340 s on a 500 MHz DEC Alpha to find the ground state of a system with 294 912 vertices (384×384 unit cells).

In addition, one can study the result of introducing a single defect pair, at given locations, into a complete matching M (a defect-free medium.) This is done by uncovering an A- and a B-vertex and arranging $|M| - 1$ dimers to cover the remaining vertices. This arrangement can be found by solving a shortest paths problem p in a directed graph G' which is determined by M and G . An undirected edge $e \in G$ is replaced with a directed edge $e' \in G'$ from the A- to a B-vertex if $e \in M$, otherwise e' is directed from the B- to the A-node. A directed path p following the edges in G' is assigned the energy change $\Delta E(p) = \sum_{e \in p} w'_e$ where $w'_e = w_e$ if $e \in M$ and $w'_e = -w_e$ for $e \notin M$. Minimal energy change paths starting from an introduced positive defect to any other vertex then give the minimal energy excitation due to a defect pair introduced at the endpoints of the path. Such paths can be determined by a shortest path (SP) algorithm that allows for negative weights; for this purpose, the Goldberg-Razik algorithm was used [14]. Note that this algorithm is distinct from the shortest paths algorithms used to study the directed polymer problem [15], where the edge weights can all be made positive by a uniform shift without affecting the paths.

Finally, the combination of the introduction of a fixed pair and defects with a chosen core energy was studied using a MWBM algorithm on a graph $G'' = (V, D \cup \{z\})$ with z an external edge connecting an A-node and a B-node at a separation $\vec{r}_{def} = (L/2, L/2)$ (in the lattice unit vector representation), with $w_z = \infty$, so that z always introduces a pair of defects separated as far as possible in a finite system. The MWBM algorithm then gives the minimum E for the introduced defects, in the presence of disorder-induced defects.

Simulations using MWBM without an introduced defect were performed for a variety of system sizes and defect core energies. The edge weights (pinning energies) were chosen from a uniform distribution in the range $[0, 1)$, with a discrete resolution of 10^{-4} . Defect densities were computed by comparing $|M|$ with the number of edges in a complete matching (a decrease in dimer number of one gives a defect pair.) Complete matching ($E_c = \infty$) configurations were compared with the partial matchings for identical disorder to determine the changes due to defects. For the largest system size (384×384 unit cells), 400 samples were studied. Simulations for introduced defect pairs using the SP algorithm were performed for systems up to 768×768 unit cells (> 4 360 samples.)

In the MWBM calculation with finite core energy, defects are readily identified as unmatched vertices (+ if a B-vertex, - if an A-vertex.) The total defect density $\rho = (N_+ + N_-)/2WL$ is fit to within statistical errors by a simple exponential, $\rho \propto \exp(-E_c/E_0)$, with $E_0 = 0.45$, for $\rho^{-1/2} > 10$. This form is consistent with the minimum core energy $E_c^{\min}(L)$ that typically excludes *introduced* defects on a length scale of L ; numerical calculation of this quantity using the SP algorithm on complete matchings gives $E_c^{\min}(L) \approx (\text{const.}) + (0.36) \ln(L)$.

The ground states with and without defects can be directly compared. There are two types of changes apparent: the introduction of vortices and changes in the matching in the regions between vortices. The changes are realized as “strings” connecting pairs of defects, as shown in Fig. 2. This result is consistent with the work of Gingras and Huse [4] who argued that in an XY model, the phase difference caused by a defect will be confined to lines connecting vortices of opposite sign. This confinement results from strong pinning on scales larger than ξ_P ; the height difference of ± 3 found on a loop enclosing a vortex is not spread out uniformly, but takes place over the scale ξ_P .

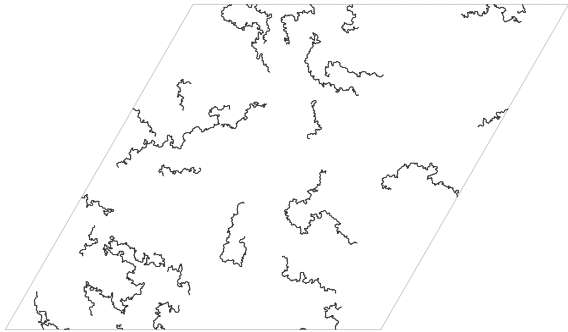


FIG. 2. The symmetric difference between matchings for a ground state with no defects and a ground state for the same disorder realization, with a defect energy of $E_c = 1.2$ (384×384 unit cells.) Dimers are included if they belong to a matching in one of the ground states, but not both. Vortices are at the ends of the defect lines. The defect lines themselves show where the phase change due to the introduction of defects is localized.

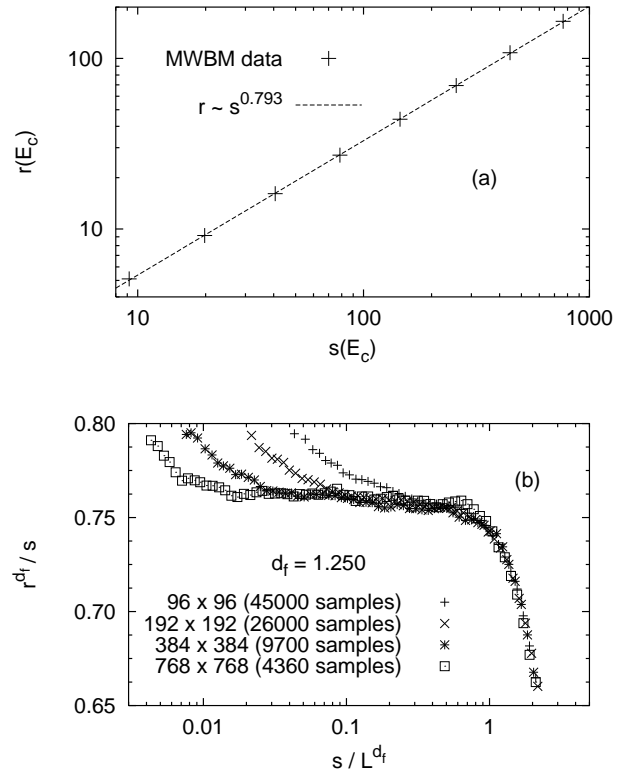


FIG. 3. (a) A plot of the mean end-to-end displacement $r(E_c)$ of defect strings vs. the mean length $s(E_c)$ of a defect path, for core energies $E_c = 0, 0.2, 0.4, \dots, 1.4$, found by examining defect strings as shown in Fig. 2. Statistical and systematic (from the extrapolation $L \rightarrow \infty$) uncertainties are less than 1% in each quantity. The straight line indicates a fit to the power law $r \sim s^{1/d_f}$, for $d_f = 1.261(16)$. (b) A finite-size scaling plot of r^{d_f}/s as a function of s/L^{d_f} from spanning trees generated by the SP algorithm on complete matchings. In this case, precise collapse over two decades with a linear abscissa gives the fitted value of d_f as $1.250(3)$.

The strings corresponding to the difference between ground states with and without defects were characterized by the string length s (number of edges in the string) and the end-to-end distance r . The mean of the end-to-end displacement distance of the paths, $r(E_c)$, and the mean length of the paths, $s(E_c)$, depends on the core energy. The dimension d_f was computed assuming

$$r(E_c) \sim s^{1/d_f}(E_c). \quad (2)$$

The quantities $r(L, E_c)$ and $s(L, E_c)$ were simply computed by averaging over all defect paths at fixed L and E_c . The limits $s(L \rightarrow \infty, E_c) = s(E_c)$ and $r(L \rightarrow \infty, E_c) = r(E_c)$ were found by scaling fits. For example, a plot of $r(L, E_c)/r(\infty, E_c)$ vs. $L/r(\infty, E_c)$ was made for trial values of $r(\infty, E_c)$ until the data collapsed to a single line. The values of $s(L, E_c)$ were scaled using a presumed scaling form $s(L, E_c)/s(\infty, E_c) \sim L/s(\infty, E_c)^{1/d_f}$, for trial values of $s(\infty, E_c)$ and d_f . The final value of d_f was

then most accurately read from a plot of $r(\infty, E_c)$ vs. $s(\infty, E_c)$, as shown in Fig. 3(a). The single defect paths caused by the two vortices placed in a complete matching, computed using the CSA and SP algorithms, were also studied. In a single sample, s can be calculated for all possible values of r ; the finite-size scaling is shown in Fig. 3(b). The fractal dimensions for the multiple defect and single introduced defect, $d_f = 1.261(16), 1.250(3)$, respectively, are numerically consistent.

The SP algorithm gives the minimum energy excitations for a pair of defects at all separations, in the absence of other defects. Applying MWBM to the extended graph G'' allows one to study a pair of defects at fixed separation in the presence of defects. The cost ΔE_{def} to introduce a defect pair is given by the difference between the ground state energies for G and G'' at the same core energy. Introducing a pair of defects, if other defects can be ignored, costs an energy $2E_c$ (for the defect cores) and a separation energy, logarithmic in the separation [5], so that at small values of $x = \rho^{1/2}L$, $\Delta E_{def} = 2E_c + c + 2\pi\gamma\rho_s \ln(L)$, where ρ_s is the long-distance stiffness associated with a single core, c is a constant, and γ is a constant given by the sample geometry. For large values of x , the introduced pair cost approaches a constant, if the disorder-induced defects screen the interaction between the introduced defects, with the crossover occurring for $\rho^{1/2}L \sim 1$ (giving $\Delta E_{def} = 2E_c + c' + 2\pi\gamma\rho_s \ln(\rho^{-1/2})$ for large x .) The results of the simulation, as plotted in Fig. (4), are consistent with this form of defect screening.

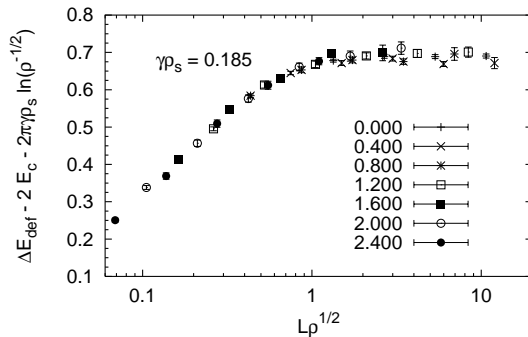


FIG. 4. A plot of the energy cost ΔE_c to introduce two maximally separated defects into a system of size $L \times L$, scaled to indicate consistency with the limits described in the text. The symbols indicate the core energy E_c ; distinct points with the same symbol are found by varying L ($L = 6, \dots, 192$.) Error bars are statistical (1σ .) The coefficient $\gamma\rho_s$ was chosen for the best scaling collapse. For fixed E_c , the defect cost approaches a constant in large systems, indicating the screening of the defect-defect interaction.

By applying optimization algorithms to many large samples, the lack of long-range elastic behavior in a disordered medium at $T = 0$ with defects is confirmed and the string dimension d_f is precisely determined. Note that

d_f appears to be distinct from the defect-step dimension 1.35 ± 0.02 previously reported [8]; this difference is surprising and further confirmation would be useful. The dimension d_f is very close to that of $5/4$ for loop-erased random walks (LERW's) [16], and distinct from the dimension $(1.22(1) [17]; 1.222(3) [18])$ of minimal-spanning trees (if the weights were all positive in G'' , the search for defect strings would give a minimal spanning tree; note that the SP algorithm has a loop-cancellation similar to that of the LERW.)

I thank Chen Zeng and Daniel Fisher for stimulating discussions of their unpublished work. This work was supported by the National Science Foundation (DMR-9702242) and by the Alfred P. Sloan Foundation.

-
- [1] Y. Imry and S.-K. Ma, Phys. Rev. Lett. **35**, 1399 (1975); A. I. Larkin and Yu. N. Ovchinnikov, J. Low Temp. Phys. **34**, 409 (1979); P. A. Lee and T. M. Rice, Phys. Rev. B **19**, 3970 (1979); T. Giamarchi and P. Le Doussal, Phys. Rev. B **52**, 1242 (1995).
 - [2] O. Narayan and D. S. Fisher, Phys. Rev. B **46**, 11 520 (1992).
 - [3] D. Cule and Y. Shapir, Phys. Rev. Lett. **74**, 114 (1995).
 - [4] M. J. P. Gingras and D. A. Huse, Phys. Rev. B **53**, 15193 (1996).
 - [5] D. S. Fisher, Phys. Rev. Lett. **78**, 1964 (1997).
 - [6] C. Zeng, A. A. Middleton, and Y. Shapir, Phys. Rev. Lett. **77**, 3204 (1996); A. A. Middleton, Phys. Rev. E **52**, 3337 (1995).
 - [7] C. Zeng, J. Kondev, D. McNamara, and A. A. Middleton, Phys. Rev. Lett. **80**, 109 (1997).
 - [8] H. Rieger and U. Blasum, Phys. Rev. B **55**, R7394 (1997).
 - [9] H. W. J. Blöte and H. J. Hilhorst, J. Phys. A: Math. Gen. **15**, L631 (1982); H. W. J. Blöte and B. Nienhuis, Phys. Rev. Lett. **72**, 1372 (1994).
 - [10] J. L. Cardy and S. Ostlund, Phys. Rev. B **25**, 6899 (1982); J. Toner and D. P. DiVincenzo, Phys. Rev. B **41**, 632 (1990); Y.-C. Tsai and Y. Shapir, Phys. Rev. Lett. **69**, 1773 (1992).
 - [11] C. Zeng, private communication.
 - [12] Source code and references can be found at <http://www.mpi-sb.mpg.de/LEDA>.
 - [13] A. V. Goldberg and R. Kennedy, Math. Prog. **71**, 153 (1995).
 - [14] A. V. Goldberg and T. Radzik, App. Math. Lett. **6**, 3 (1993).
 - [15] D. A. Huse and C. L. Henley, Phys. Rev. Lett. **54**, 2708 (1985); M. Kardar and Y.-C. Zhang, Phys. Rev. Lett. **58**, 2087 (1987).
 - [16] S. Majumdar, Phys. Rev. Lett. **68**, 2329 (1992).
 - [17] M. Cieplak, A. Maritan, and J. R. Banavar, Phys. Rev. Lett. **76**, 3754 (1996).
 - [18] A. Alan Middleton, unpublished. Determined by similar scaling plots for minimal spanning trees ($\leq 1100^2$).